Published in Journal of Volcanology and Geothermal Research 170, issues 3-4, 153-166, 2008
which should be used for any reference to this work

Multiple caldera collapses inferred from the shallow electrical resistivity signature of the Las Cañadas caldera, Tenerife, Canary Islands

Nicolas Coppo [a], Pierre-André Schnegg [a,*], Wiebke Heise [b], Pierik Falco [a], Roberto Costa [a]

[a] *Geomagnetism Group, Department of Geology, University of Neuchâtel, 11 rue Emile-Argand, CP 158, 2009 Neuchâtel, Switzerland*
[b] *GNS Science, P.O. Box 30368, Lower Hutt, New Zealand*

Abstract

The Las Cañadas caldera of Tenerife (LCC) is a well exposed caldera depression filled with pyroclastic deposits and lava flows from the active Teide–Pico Viejo complex (TPVC). The caldera's origin is controversial as both the formation by huge lateral flank collapse(s) and multiple vertical collapses have been proposed. Although vertical collapses may have facilitated lateral slope failures and thus jointly contribute to the exposed morphology, their joint contribution has not been clearly demonstrated. Using results from 185 audiomagnetotelluric (AMT) soundings carried out between 2004 and 2006 inside the LCC, our study provides consistent geophysical constraints in favour of multiple vertical caldera collapse. One-dimensional modelling reveals a conductive layer at shallow depth (30–1000 m), presumably resulting from hydrothermal alteration and weathering, underlying the infilling resistive top layer. We present the resistivity distribution of both layers (resistivity images), the topography of the conductive layer across the LCC, as well as a cross-section in order to highlight the caldera's evolution, including the distribution of earlier volcanic edifices. The AMT phase anisotropy reveals the structural and radial characteristics of the LCC.

Keywords: audiomagnetotellurics; caldera; hydrothermal alteration; conductive layer; Tenerife

1. Introduction

The Las Cañadas caldera (LCC) (Fig. 1) is one of the best exposed calderas in the world (size: 16 × 9 km) and part of the central volcanic complex (CVC) on Tenerife. However, its origin is controversial and the debate is centred around whether the depression resulted from lateral or vertical collapses. Numerous studies argue that the present caldera wall scarp was produced by one or several lateral flank collapses directed towards the north (Bravo, 1962; Navarro and Coello, 1989; Ancochea et al., 1990; Carracedo, 1994; Watts and Masson, 1995; Ancochea et al., 1998; Watts and Masson, 1998; Ancochea et al., 1999; Cantagrel et al., 1999; Arnaud et al., 2001; Watts and Masson, 2001; Masson et al., 2002). Another line of arguments relates to the LCC's formation as a result from repeated vertical collapses produced by roof collapse during major caldera-forming volcanic eruptions (Fúster et al., 1968; Araña, 1971; Marti et al., 1994a; Marti et al., 1996; Marti et al., 1997; Bryan et al., 1998; Marti, 1998; Marti and Gudmundsson, 2000).

Although a growing number of combined geological and structural information point towards a vertical collapse origin (Marti et al., 1994a; Marti and Gudmundsson, 2000), there is no detailed sub-surface geophysical data of the entire caldera that unambiguously support this hypothesis. Only two MT studies have so far been performed to investigate the electrical properties of the caldera fill (Ortiz et al., 1986; Pous et al., 2002). At shallow depth, a resistive layer (unaltered or "fresh" lava) overlies a conductive layer (hydrothermalised lava), both of which also crop out at the surface (Fig. 2).

In order to shed light on the caldera's origin, a dense high-resolution audiomagnetotelluric (AMT) survey has been carried

* Corresponding author. Tel.: +41 32 718 26 76; fax: +41 32 718 26 01.
E-mail addresses: nicolas.coppo@unine.ch (N. Coppo), pierre.schnegg@unine.ch (P.-A. Schnegg), w.Heise@gns.cri.nz (W. Heise), pierik.falco@net2000.ch (P. Falco), roberto.costa@unine.ch (R. Costa).

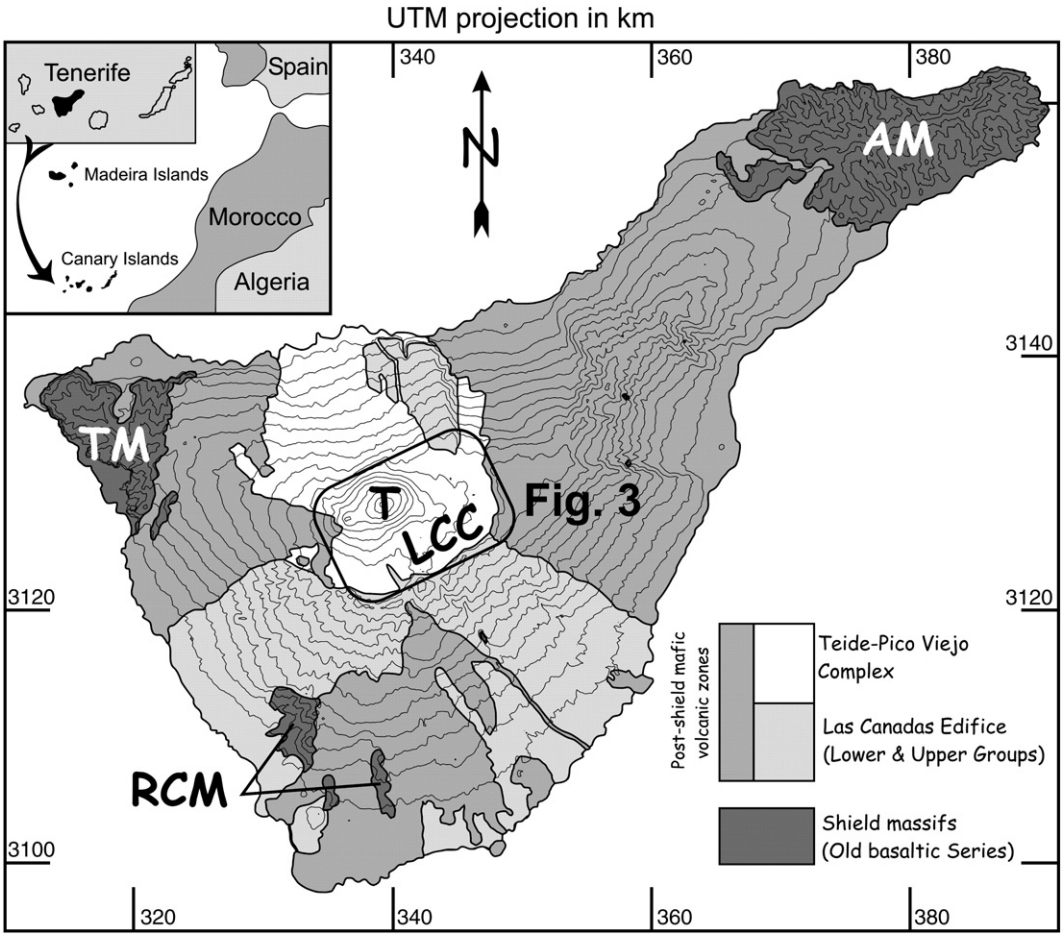

Fig. 1. Simplified geological map of Tenerife (Canary island). The three old basaltic series are: Anaga Massif (AM), Teno Massif (TM) and Roque del Conde Massif (RCM). Rotated central rectangle (Fig. 3) shows the study area, the Las Cañadas caldera (LCC) with the Teide volcano (T).

out. Here we report on results from 185 soundings performed inside the area bounded by the LCC scarp wall. We present results on the internal shallow structure of the LCC (depths between 0 and 2000 m below the surface) in an effort to extend our knowledge on the interior architecture of the CVC. We provide: (1) electrical resistivity maps and constrain the thicknesses and topography of two major lithological layers; (2) an interpretation of hydrothermal processes occurring at the LCC; and (3) a structural interpretation of our results and their implications for the formation of the LCC.

2. Audiomagnetotelluric (AMT) method and specifications

The magnetotelluric (MT) method is a passive surface geophysical technique, which uses the Earth's natural EM fields to investigate the electrical resistivity distribution at depth, from

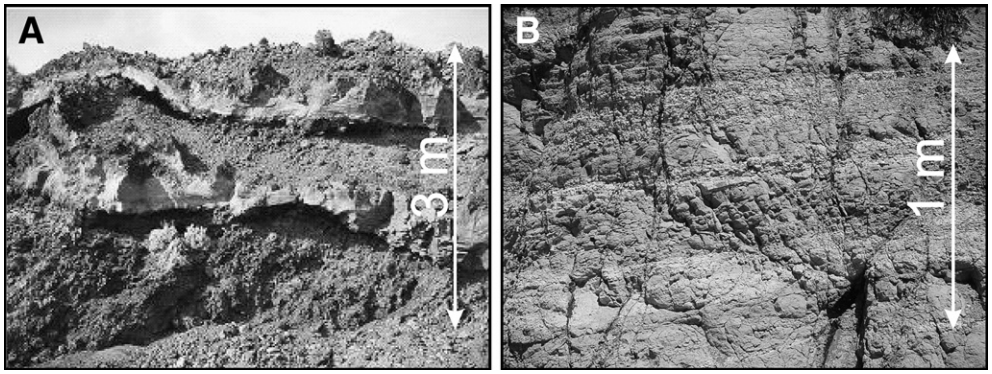

Fig. 2. A) "Fresh" lava and pyroclastic flows — resistive layer. B) Hydrothermalised clay-rich lava — conductive layer.

tens of metres to tens of kilometres depth (Vozoff, 1991). The AMT technique uses higher frequencies (above 1 Hz) generated by thunderstorm activity around the world. Currently, MT and AMT methods are widely used in many domains of pure and applied geophysics such as mineral and geothermal reservoir exploration as well as for the investigation of the internal structure of volcanoes (Benderitter and Gérard, 1984; Ballestracci and Nishida, 1987; Benderitter, 1987; Courteaud et al., 1997; Schnegg, 1997; Fuji-ta et al., 1999; Matsushima et al., 2001; Savin et al., 2001; Pous et al., 2002; Volpi et al., 2003; Manzella et al., 2004). The MT theory was well presented in the pioneering paper of Cagniard (1953) or related papers and further details are given in Simpson and Bahr (2005).

We used an AMT recording system developed at the University of Neuchâtel (Switzerland), light enough to be carried by a crew of two. The four horizontal components were sampled at 2 kHz during 8 min in the NS and EW direction and in the period range 0.001 to 0.3 s. Two 50 m long telluric lines were arranged orthogonally and connected to non-polarizing electrodes made of acrylic tubes covered either end by porous ceramic. Inside the tube a non-polarizing Ag–AgCl slat designed for ocean studies (Filloux, 1987) was immersed in a saturated KCl solution leaking through the ceramic. Two horizontal magnetic induction coils (ECA CM16) were installed orthogonally to each other within the area marked by the telluric lines.

Field campaigns were carried out between 2004 and 2006 (164 AMT soundings). 21 of the 33 AMT soundings presented in Pous et al. (2002) were also employed in our study (Fig. 3).

3. Geological and geophysical setting

3.1. Geological setting

Tenerife, the largest island of the Canarian archipelago, lies a few hundred kilometres off the African coast (Fig. 1). It is home to the second largest oceanic island volcanic complex in the world after Mauna Loa and Mauna Kea in Hawaii. The subaerial portion of the island known as the Old Basaltic Series (Fúster et al., 1968), is a composite mafic alkaline formation constructed by fissure eruptions of ankaramites, basanites and alkali basalts between 12 and 3.5 Ma (Abdel-Monem et al., 1972; Ancochea et al., 1990) and now preserved at the three corners of the islands: the Anaga peninsula (NE), the Teno massif (NW), and the Roque del Conde (S) (Fig. 1). Toward the end of this period, volcanic activity concentrated in the central part of Tenerife, where shallow phonolitic magma chambers developed to form a central volcanic complex, the Las Cañadas edifice (LCE). Of basaltic to phonolitic composition, it was constructed and modified by several volcanic cycles (Araña, 1971; Ancochea et al., 1990; Marti et al., 1994a; Ancochea et al., 1998; Ancochea et al., 1999).

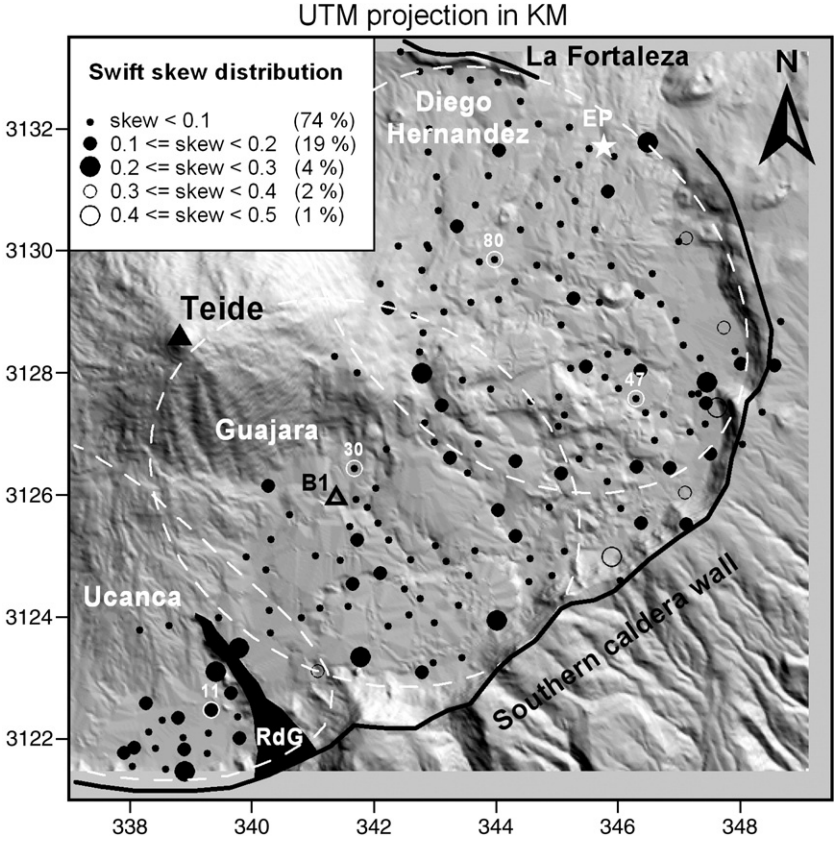

Fig. 3. Swift skew (185 AMT soundings) distribution inside the Las Cañadas caldera. Location of 4 AMT sites (small white circles) presented on Fig. 4. Location of the three calderas thought to have built the current LCC (dotted white ellipses). RdG: Roques de Garcia. B1: borehole B1 (Ablay and Marti, 2000). EP: El Portillo.

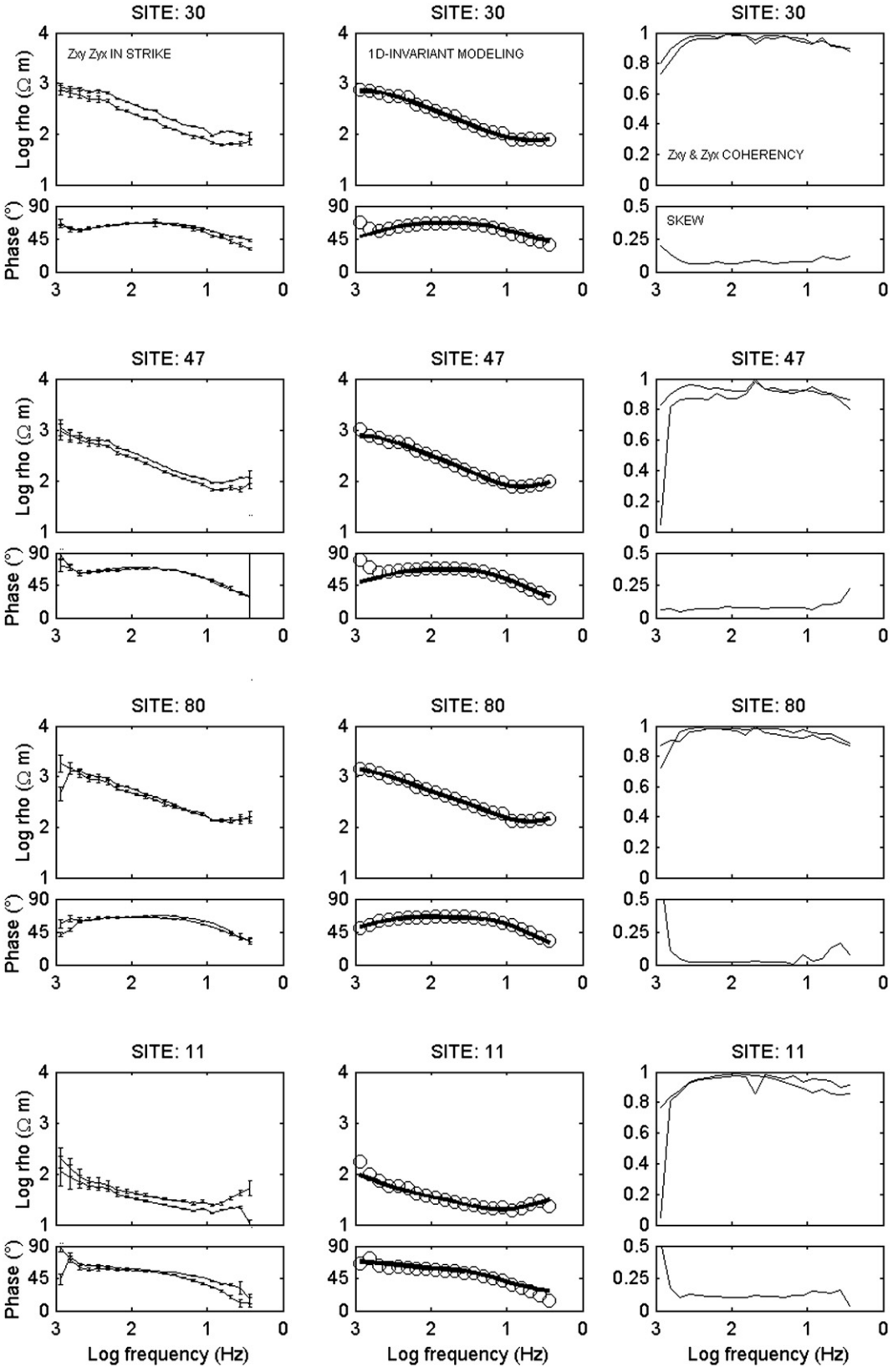

Fig. 4. Four AMT soundings (30, 47, 80, 11). (a) Apparent resistivity, phase for both Zxy and Zyx vs. period in strike direction given by the maximum phase anisotropy. b) 1-D invariant modelling. c) Coherency functions and skewness. The three first sites are typical 1-D, the 4th is slightly affected by 2D effect.

Following Marti et al. (1994a), the LCE includes a complex and poorly studied Lower Group (3.5–2 Ma), and an Upper Group (1.6–0.17 Ma). The Lower Group includes up to 7 units mainly cropping out in the lower parts of the caldera wall, and is composed of phonolitic, basaltic lava and minor pyroclastic rocks, including phonolitic welded tuff. Amongst the units described by Marti et al. (1994a) is the Roques de Garcia Sequence which defines an isolated spur from the caldera wall towards the TPVC, composed of primary and reworked volcanic rocks, mainly lithic-rich ignimbrites, breccias and megabreccias, and minor phonolitic lava. The Upper Group consists of three formations: Ucanca (1.54–1.07 Ma), Guajara (0.85–0.57 Ma) and Diego Hernandez (0.38–0.18 Ma), each of which ended by caldera collapse (Marti et al., 1994a; Marti et al., 1997) (Fig. 3). This overlapping collapse process is attributed to the eastward migration of a shallow magma chamber (Marti and Gudmundsson, 2000). The Ucanca Formation is mainly composed of phonolitic lava and pyroclastic rocks, many of them welded tuffs, but also basaltic lava. The Guajara Formation consists of welded tuffs, non-welded pyroclastic rocks, and some basaltic lava. The Diego Hernandez Formation is formed by non-welded pyroclastic rocks, mainly ignimbrites, and basaltic lava. The rocks of both the Lower and the Upper Groups are intruded by inclined sheets dipping towards the centre of the caldera depression, sub-vertical dykes, and plug intrusions of phonolitic composition.

3.2. Previous geophysical studies

Although the LCC has been the target of several geophysical studies at different scales over the past 30 years (MacFarlane and Ridley, 1968; Viera et al., 1986; Camacho et al., 1991; Aubert and Kieffer, 1996; Camacho et al., 1996; Aubert and Kieffer, 1998; Ablay and Kearey, 2000; Araña et al., 2000), only two MT surveys have so far investigated its electrical structure.

The first MT survey confirmed the existence of a double tectono-volcanic depression inside the LCC partly filled by coarse material and lava and expressed the possibility that geothermal fluids may circulate under the central area of the eastern sector at relatively shallow depths (Ortiz et al., 1986). In addition, they interpreted a deep conductive horizon detected at 13 km beneath the LCC as the Moho discontinuity.

The second MT and AMT study identified two closed depressions in the western (Ucanca) and central (Guajara) sectors, and a gentle inclination of the top of the main conductive zone towards the northeast (La Orotava Valley) in the eastern sector (Diego Hernandez) of the LCC (Pous et al., 2002). They highlighted the presence of a narrow and marked conductive anomaly running parallel to the present caldera wall, suggesting the presence of the structural border of the caldera. Based on resistivity data, they postulated two main aquifer zones separated by the Roques de Garcia and proposed the

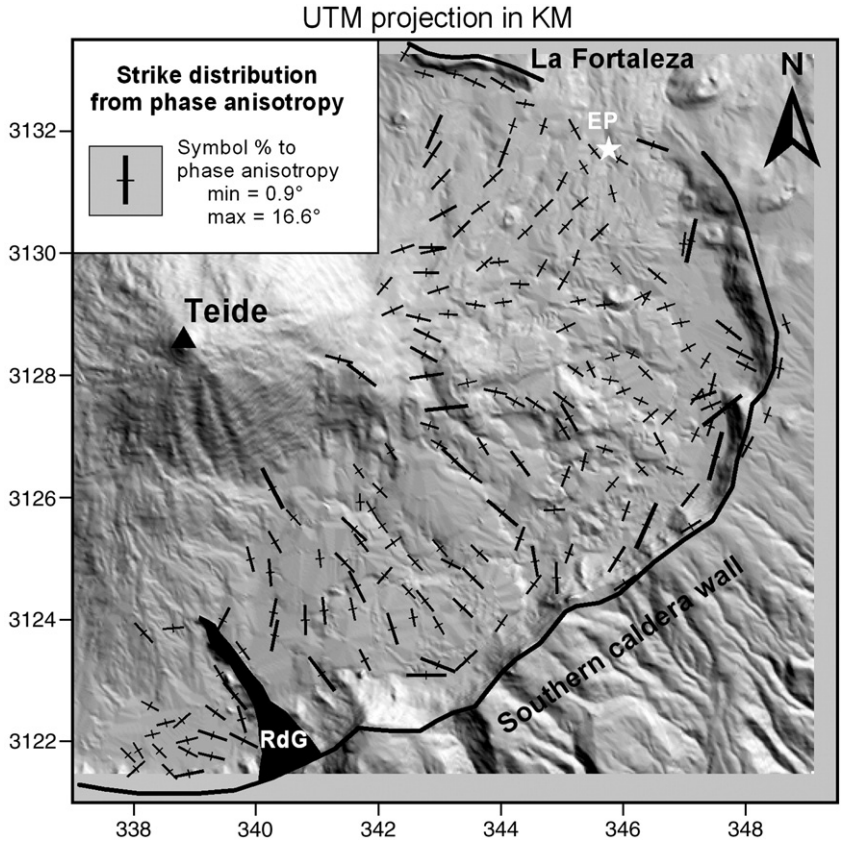

Fig. 5. Strike distribution from maximum phase anisotropy. Ambiguity of 90° is indicated by the smallest branch. The largest is proportional to the phase anisotropy; minimum = 0.9° and maximum = 16.6°.

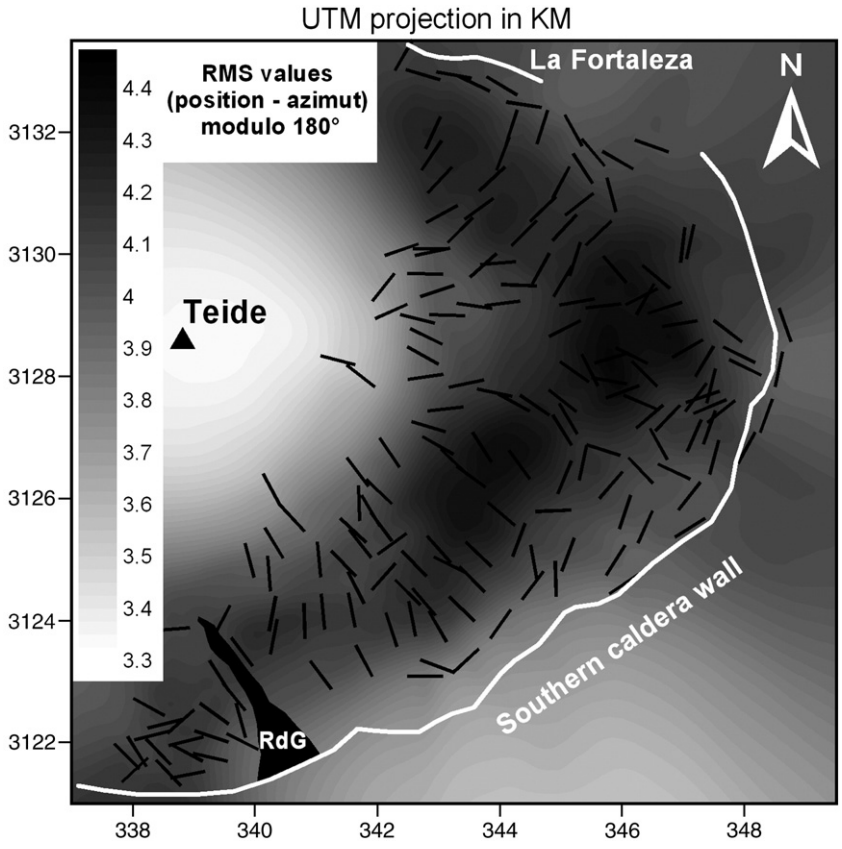

Fig. 6. Spatial distribution of the RMS between AMT site position and their strike azimuth modulo 180°. Here, the centre of TPVC (smallest RMS) appears to be the only body responsible for the observed strike distribution.

presence of another buried structural feature separating the eastern (Diego Hernandez) and central part (Guajara) of the LCC, in accordance to the postulated overlapping collapse origin proposed by Marti and Gudmundsson (2000).

4. Results

4.1. Dimensionality and modelling

The locations of the AMT sites collected in the eastern sector of the LCC are shown in Fig. 3 and following. Except for a few soundings affected by cultural EM disturbances, the overall data quality is very good and allows accurate estimation of the transfer functions. Most of the data show a uniform, close to 1-D behaviour and display similar results in the whole area, in good agreement with Pous et al. (2002). The shape of the apparent resistivity and phase curves reveals a resistive layer overlying a conductive layer (Fig. 4). At times a third layer appears at depth, enabling an estimation of the thickness of the conductive layer. However, we focus on the thickness of the first layer and the resistivity of the two first layers.

Only a few soundings display curve splitting at higher and lower frequencies due to shallow heterogeneities and due to signal weakness (Fig. 4, 4th site). In order to validate the 1-D modelling approach for all sites, including those located close to the caldera wall, we performed a forward modelling. Results and field observations are in good agreement and validate the use of the simplified 1-D approach to track the shallow internal architecture of the LCC. Likewise, 2-D inversions computed on profiles radial to the Teide volcano confirm this approach. Recently, 3-D model results indicated that ocean effect significantly influences the signal at about 4–6 s for the phase and 20 s for the apparent resistivity in the LCC (Pous et al., 2002). Similar results have recently been reported by Monteiro Santos et al. (2006).

The Swift skew (Swift, 1967) is the ratio between the magnitudes of the diagonal and off-diagonal components of the MT impedance tensor, which provides an ad hoc measure of the MT impedance tensor's proximity to an ideal 2-D impedance tensor, for which the diagonal components are expected to vanish (Simpson and Bahr, 2005). Our results show that 74% of the sites display a mean Swift skew below 0.1, 19% between 0.1 and 0.2, 4% between 0.2 and 0.3, 2% between 0.3 and 0.4 and 1% above 0.5 (Fig. 3). Most of the sites with Swift skew values above 0.2 are found along the southern caldera wall. This suggests a more complex 2-D to 3-D structure related to the rise of the conductive layer along the wall. However, there are also many soundings with Swift skew lower than 0.2. From a number of Very-Low Frequency EM (VLF-EM) profiles carried out during this study in the LCC, it became apparent that a metallic pipe or cable is buried close to the caldera wall along the track from Las Angosturas to El Portillo. Another visible pipe collecting groundwater from Montaña Guajara crosses the caldera floor close to the Parador Hotel. These pipes or cables

generate EM disturbances along the caldera wall. These artifacts may explain both the higher Swift skews observed along the caldera wall and the bad quality of some AMT and MT data collected in this area by Pous et al. (2002) and by the authors during the first campaign in 2004.

Finally, invariants of all AMT soundings have been modelled separately (Fig. 4) using a 1-D modelling scheme (Fischer and Le Quang, 1981; Schnegg, 1993). Then, subtracting the thickness of the first resistive layer from the altitude, new elevations were interpolated to visualise the topography of the conductive layer (Fig. 9). Likewise, resistivity values were interpolated to obtain the resistivity distribution of the first and second layers (Figs. 7 and 8).

4.2. Static shift effect

The magnetotelluric (MT) static shift is a galvanic distortion effect that affects locally apparent resistivity sounding curves by shifting them by a scaling factor independent of the frequency, keeping the phases unchanged (Simpson and Bahr, 2005). This effect is due to charge accumulation at boundaries of shallow conductive heterogeneities, disturbing locally the regional electric field. The rotation of our impedance tensors reveals that several soundings display a static shift effect, generally small but sometimes reaching up to 1 decade. To remove this effect we applied a geostatistical method based on co-kriging. This technique uses the spatial distribution of the measured apparent resistivity and phases at a few selected frequencies, and their known intrinsic correlation, to compute a static shift-free estimate of the apparent resistivity (Tournerie et al., 2007). Further details on the method and its applications on this data set are reported in Tournerie et al. (2007).

4.3. Strike distribution in a near 1-D environment

In spite of a general 1-D behaviour, our data exhibit some 2-D anisotropy. Since the apparent resistivity can be affected by static shift in an unknown fashion, we used only the phase for our analyses. Rotating the impedance tensor and looking for the maximum phase anisotropy (mean value over the 15 central periods 2.7×10^{-03} to 1.5×10^{-01} s), we obtained consistent results for the strike distribution of the anisotropy (Fig. 5). The period interval has been chosen to discard erroneous values observed at some stations and generated by noisy EM signals. From these results, it can be observed that strikes, except for the western part (Ucanca caldera), are radially distributed around the TPVC, or parallel to the southern caldera wall.

We compute the RMS angular difference between the direction of each sounding and the azimuth of the MT tensor modulo 90° and 180° azimuths given by the phase anisotropy at each grid point (spacing 50 m) covering the LCC floor in order to identify potential geological causes for the observed anisotropy.

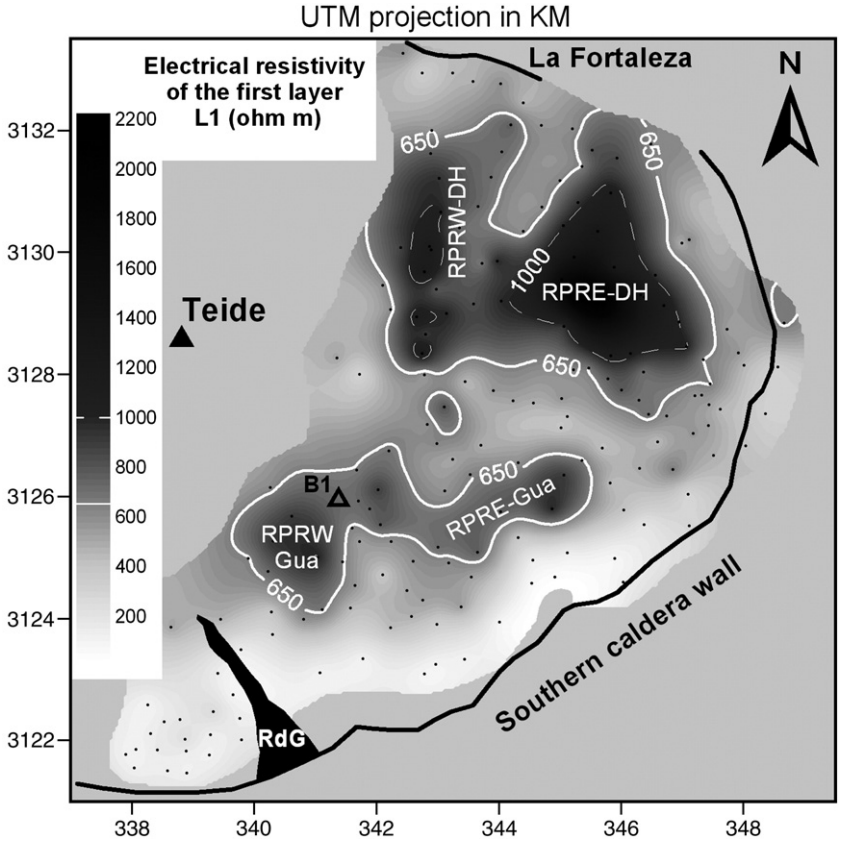

Fig. 7. Resistivity distribution of the first resistive layer. Isolines 650 and 1000 Ωm are drawn in white. Black points are AMT sites. RPRW-Gua and RPRE-Gua: Western and Eastern Resistivity Prints of the Resistive layer (Guajara). RPRW-DH and RPRE-DH: Western and Eastern Resistivity Prints of the Resistive layer (Diego Hernandez).

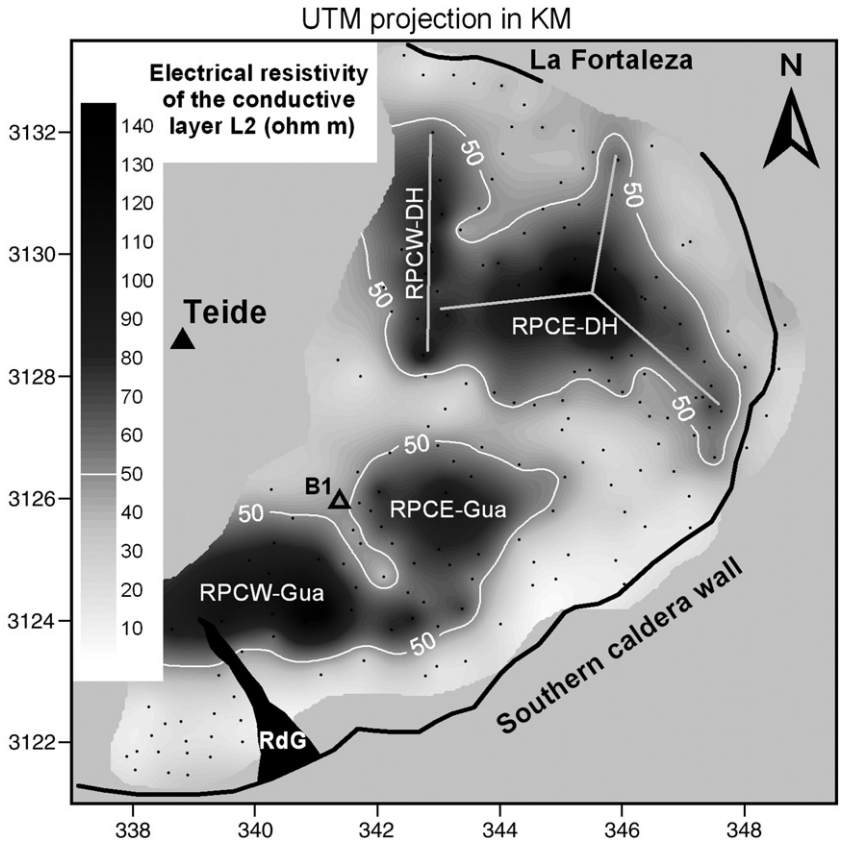

Fig. 8. Resistivity distribution of the conductive layer. Isoline 50 Ωm are drawn in white. Black points are AMT sites. RPCW-Gua and RPCE-Gua: Western and Eastern Resistivity Prints of the Conductive layer (Guajara). RPCW-DH and RPCE-DH: Western and Eastern Resistivity Prints of the Conductive layer (Diego Hernandez). Plain grey lines: postulated structural trends of the Diego Hernandez conductive print.

Fig. 6 shows the spatial distribution of the RMS. Minima indicate locations potentially responsible for the observed strike. The absolute minimum appears on the 180° map and is identified as the centre of the TPVC.

4.4. Resistivity distribution

Fig. 7 shows the spatial distribution of the electrical resistivity of the caldera fill (first layer). Products of the TPVC (Ablay and Marti, 2000) form the majority of the in-fill lithologies that today cover all three caldera depressions forming the LCC (Marti et al., 1994a). Electrical resistivity values range from 10 Ωm to 2100 Ωm all over the LCC. The most conductive zone runs parallel to the southern caldera wall where the underlying conductive layer appears to be very close to the surface. Two main areas with resistivities in excess of 650 Ωm may be distinguished. They are referred to in the following as "resistivity prints of the resistive layer" (RPR) of both the Guajara (Gua) and the Diego Hernandez (DH) calderas, respectively. RPR-Gua is exactly located in the Guajara sector of the LCC. The second maxima coincides with the Diego Hernandez sector of the LCC believed to have formed by the latest vertical caldera collapse (Marti et al., 1994a). They are separated by some hundred metres of more conductive rocks aligned in the direction of the Santiago del Teide ridge (NW–SE). We note that borehole B1, located in the middle of RPR-Gua (Fig. 7, black triangle) only encountered PT-PV lithologies over its entire 510 m depth, without penetrating pre-caldera rocks (Ablay and Marti, 2000).

The resistivity distribution of the conductive layer is more homogeneous than that of the resistive layer (Fig. 8). Resistivities range from 10 to 150 Ωm and highlight two main electrical prints (50 Ωm isolines), located in the Guajara and Diego Hernandez calderas. They are referred to in the following as "resistivity prints of the conductive layer" (RPC) of both the Guajara (Gua) and the Diego Hernandez (DH) calderas, respectively. Although locations are similar to those of the resistive layer, their morphologies are quite different, especially for the case of Guajara. The southern print is located in the Guajara caldera. It can be divided into 2 smaller areas separated by a narrow, higher-conductivity feature: a western sector (here referred to as RPCW-Gua), and an eastern one (RPCE-Gua). The northern print is located in the Diego Hernandez (RPC-DH) sector. The RPC-DH and RPR-DH may be divided into an eastern triangular shape (RPCE-DH and RPRE-DH) and a more elongated western sector (RPCW-DH and RPRW-DH).

4.5. Morphology of the top-most conductive layer

Knowledge of the shape and depth of the interface between resistive and conductive rocks is of great importance not only

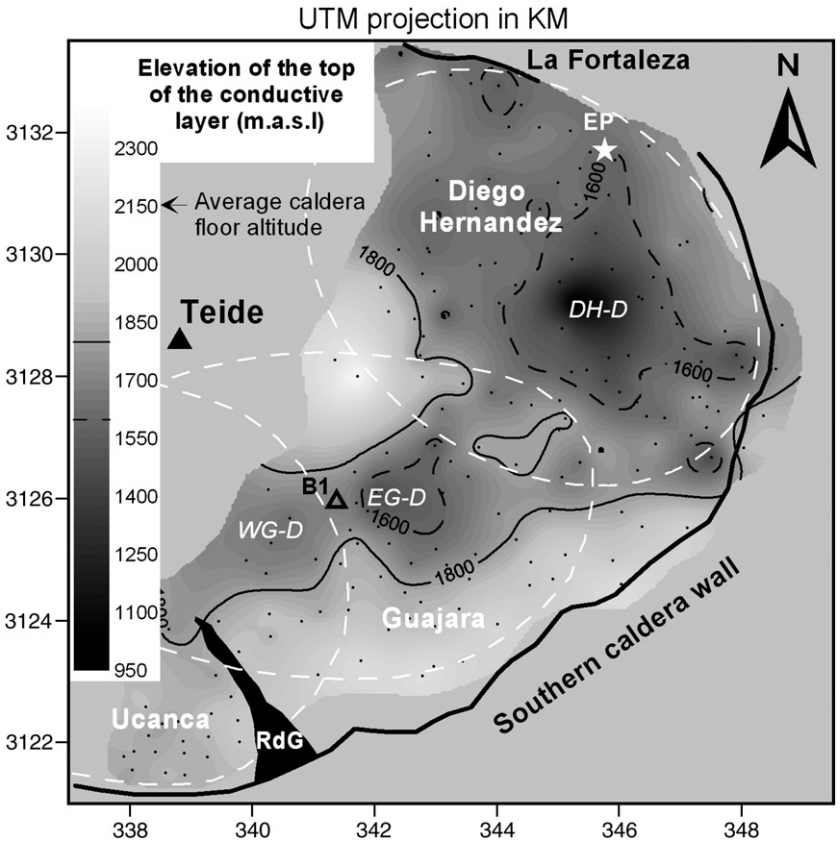

Fig. 9. Interpolated altitude of the top conductive layer as revealed by the 185 AMT soundings. Isolines 1600 and 1800 m.a.s.l. are drawn in black. Black points are AMT sites. Inferred locations of the three calderas (dotted white ellipses) at the origin of the current LCC.

due to its hydrogeological implications but also for structural constraints on the origin of the LCC. After removing the thickness of the first resistive layer from the elevation of each AMT site, we interpolate a new datum of altitudes shown in Fig. 9. The enhanced conductivity of the second layer is assumed to originate from hydrothermal alteration. As this process requires time, the top-most conductive layer can be considered an interface between older and younger rocks. Tracing its topography we note that its surface is inclined towards the NE. Two funnel-shaped structures are found between more conductive borders marked to the south by the caldera wall and to the north by the current TPVC. We note a steeper slope of the conductive layer in the northern part of the LCC, which is believed to be a consequence of the hydrothermal activity of the recent TPVC. The southern conductive zone runs parallel to the LCC wall from Ucanca to El Portillo (Fig. 9). Its extension is much wider than previously estimated by Pous et al. (2002) and shows a clear reduction in width along the southern and eastern sides of Diego Hernandez wall.

The eastern-most elliptical depression, presumably related to the Diego Hernandez caldera (here abbreviates DH-D (Fig. 9) for Diego Hernandez depression), has its main axis orientated NNW–SSE. Its northern part is flatter than the southern one. Its lowest altitude is 1150 m.a.s.l. and is more or less centrally located above the Dorsal rift extension. The limit of this depression is quite well constrained, except in a small area in the NW part.

The more circular central depression, assigned to the Guajara caldera, has a minimum altitude of 1550 m.a.s.l. and is referred to as the eastern Guajara depression (EG-D, Fig. 9). In its western part, it could include a second depression with a minimum altitude of 1650 m.a.s.l., here referred to as the western Guajara depression WG-D. The limit between DH-D and EG-D is well marked. It runs parallel to the SE extension of the Santiago del Teide ridge. This boundary marks an elongated structure with a maximum altitude of 1800 m.a.s.l. A borehole B1 (Fig. 9) is located at the boundary between WG-D and EG-D, where the top-most conductive layer reaches 1700 m.a.s.l.

In the western-most Ucanca sector of the LCC, the conductive layer appears to be at very shallow depth (~100 m.), in good agreement with previous studies and borehole data (Ablay and Marti, 2000; Pous et al., 2002).

5. Discussion and interpretations

5.1. Strike distribution and structural pattern of the LCC

The radial strike distribution (Figs. 5 and 6) results from geological structures related to the growth of the TPVC. Two points are noteworthy.

First, the radial pattern of lava and pyroclastics infilling the LCC around PV-PT to a depth of 510 m (Ablay and Marti, 2000). The gentle cone-like structure over which they flowed induces small 2-D effects observed in the phase. Field

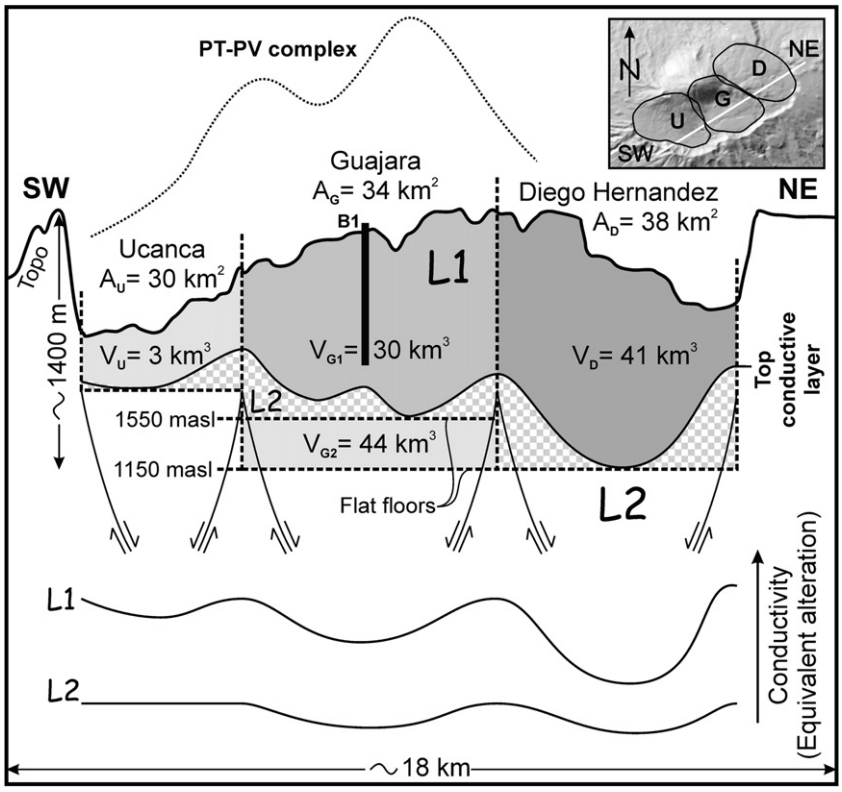

Fig. 10. SW–NE schematic cross-section through the LCC. Inset: cross-section and sub-caldera location. L1 = resistive lava from the TPVC; the darker the grey, the higher the resistivity (Fig. 7). L2 = conductive and altered rocks at depth. Both layers are limited by the top conductive layer (black line). A_x = planar areas of the three sub-calderas. V_x = volumes of resistive rocks computed for the 3 sub-calderas between the topography and a simplified flat floor (vertical and horizontal dashed lines). $V_{G2} = V_{G1} + 14$ km^3. See text for explanation regarding the additional volume (14 km^3) below Guajara caldera. B1 = 510 m deep borehole.

observations indicate that soils and vegetation of the LCC develop more easily where volcanoclastic material is finer (pumices, ashes) than in the middle of lava flows. Once these soils are covered with lava flows, they constitute small conductive zones, generally oxidised, locally known as “almagres” or paleosoils (Caloz, 1987). Outwards dipping away from the TVPC and radial to it, they may induce the small 2-D effects observed.

Secondly, intruding dikes related to the TPVC together with local extensional and circumferential stress-fields (Ablay and Marti, 2000) may also cause radial anisotropy. Radial vent alignment exposed in the Guajara sector serves as an example. Recent laboratory experiments show that radial faults and/or dike injection, can form both during inflation or deflation and collapse of a magma chamber (Gudmundsson, 1988; Marti et al., 1994b; Walter and Troll, 2001). During its evolution, the TPVC may have experienced multiple inflation and deflation cycles which may generate such structural patterns.

The second main structural feature influencing some soundings (Figs. 5 and 6) runs parallel to the caldera wall. It results from the presence of the conductor at shallow depth and its inward (away from the wall) dipping slope. The origin of the conductor from caldera ring is attributed to faults marking a large fracture network that favoured rock hydrothermalisation.

Strikes of soundings located close to the La Fortaleza wall clearly indicate the presence of a structure parallel to the LCC wall. A similar orientation can also be observed towards El Portillo suggesting the buried continuation of this geological feature at the head of the Orotava Valley. Our results support the association of the La Fortaleza scarp with the LCC wall and it should hence be seen as the continuation of the eastern caldera wall formed during the Diego Hernandez caldera collapse (Marti et al., 1994a). At La Fortaleza, the top-most conductive layer extends to about 400 m below the surface, in good agreement with data from borehole B2 which penetrated 360 m of recent lava without reaching pre-caldera rocks (Ablay and Marti, 2000).

5.2. Hydrothermal alteration and resistivity prints

Shallow conductive zones in volcanic areas are interpreted to result from hydrothermal alteration, geothermal systems (saline groundwater) (Benderitter and Gérard, 1984; Ballestracci et al., 1985; Matsushima et al., 2001; Savin et al., 2001; Pous et al., 2002; Zlotnicki et al., 2003; Manzella et al., 2004; Revil et al., 2004; Aizawa et al., 2005; Monteiro Santos et al., 2006). Of low permeability (Courteaud et al., 1997; Descloitres et al., 1997), these conductive bodies are also seen as cap rocks, aquicludes or seawater intrusions (Müller and Haak, 2004). The conductive zones highlighted in this study are most likely a result from hydrothermal alteration along ring faults and a complex pattern of conjugate faults (Galindo et al., 2005). Coloured, clay-rich

and compact rocks outcropping in the Los Azulejos graben in the LCC depict hydrothermally altered rocks expected to be found at depth (Fig. 2).

We propose that the resistivity distribution of the top-most two layers (Figs. 7 and 8) points towards the existence of 2 buried volcanic structures in the LCC. We use the term "resistivity print" to describe the homogeneous and consistent effects of hydrothermal alteration over large areas through time. Resistivity prints have to be seen as isolines of hydrothermal alteration and therefore as a state of a specific alteration intensity at a point in time.

5.3. Interpretation of Diego Hernandez caldera

Rift zones on Tenerife and have often been reported to form two- or three-armed rifts (Carracedo, 1994; Walter and Schmincke, 2002) with significant dyke intrusion and faulting along them (Marinoni and Gudmundsson, 2000). In Tenerife, three rift axes have been identified (Carracedo, 1994; Walter and Troll, 2003). The most prominent rift displays a NE–SW trend (the Dorsal ridge) and connects the Anaga massif to the LCC (Fig. 1). The second one has a NW–SE trend (the Santiago del Teide ridge) and connects the Teno massif to the LCC. Below, we interpret the morphologies of the RPR-DH and RPC-DH as a consequence of the orientation of these rift zones (Figs. 7 and 8). Although controversial, we show that the third SSW–NNE trend would have been effective during Diego Hernandez volcanic cycle.

Both RPR-DH and RPC-DH show an elongated feature orientated NNE–SSW in the east and a triangular morphology in the west (Figs. 7 and 8). The triangular morphology suggests the existence of an old volcanic edifice while the elongated structure supports the existence of a lineament feeding volcanic eruptions. This volcanic double structure points to the presence of multiple magma chambers from which two major phonolitic eruptions were fed throughout the eruptive history of the Diego Hernandez formation (Edgar et al., 2007). The three dominant orientations (Fig. 8) of the triangular features are NNE–SSW, SE–NW and WSW–ENE and thus appear to be slightly rotated off the axes of the current three rifts.

The SE–NW trending conductive structure that separates RPRW-DH and RPRE-DH (Fig. 7) or RPCW-DH and RPCE-DH close to La Fortaleza wall sheds light on the formation of the Diego Hernandez depression. The low resistivity signature, comparable to that found along the caldera, suggests that this structure is part of a ring fault activated during the caldera-forming eruption related to the Diego Hernandez collapse. This would imply that the formation of the eastern-most sector of the LCC (Diego Hernandez sector) was to some extend controlled by the main structural feature of the SW–NE trending Dorsal ridge. The Diego Hernandez conductive structure is comparable to the conductive spur separating the RPC-Gua into the RPCW-Gua and RPCE-Gua sectors.

Another conductive zone is located below the La Fortaleza wall and although the wall scarp is lower than the southern LCC wall, it appears to be related to the vertical collapse of the northern part of the Diego Hernandez caldera.

The top-most conductive layer is characterised by a funnel-like depression (below 1600–1650 m.a.s.l. (Fig. 9)) with an opening towards the north, in agreement with (Aubert and Kieffer, 1998; Pous et al., 2002). The depression almost reaches the missing wall segment at El Portillo. From both the resistivity prints and the morphology of the conductive layer, we suggest that the vertical collapse initiated in the SE part of the Diego Hernandez caldera below the main LC edifice. The main collapse however was controlled by the major SW–NE trending tectonic lineament. Propagating northwards, we postulate that the collapse subsequently triggered the giant Icod landslide at the north of the LC edifice (Marti et al., 1997; Hürlimann et al., 2000). This hypothesis is also supported by results of an AMT profile along the northern flank of the TPVC (Coppo et al., in press, submitted) that shows a 1 km deep buried incision in this area, orientated NNW seawards.

In comparison to the Guajara sector, the thinner conductive zone bordering the Diego Hernandez caldera (Figs. 7 and 8) is explained by its younger age, resulting in a less effective hydromineralisation over time. This provides additional geophysical evidence for the hypothesis of separate vertical collapse events as the origin of the LCC (Marti et al., 1994a; Marti and Gudmundsson, 2000).

5.4. Interpretation of Guajara caldera

While RPR-DH and RPC-DH enable an interpretation of the structural features (see above) implied during Diego Hernandez volcanic cycle, the morphology of RPR-Gua and RPC-Gua does not enable an accurate determination of the original Guajara structural trends. Thus, we only point out the clear SW–NE trend (Figs. 7 and 8).

The conductive spur (Fig. 8) between RPCW-Gua and RPCE-Gua is thought to be the limit of an old composite volcano formed by two closely-spaced volcanic edifices comparable to the present TPVC. It may also be the result of a strong hydrothermal alteration related to the southern felsic Teide vent alignment in Guajara caldera. The two hypotheses do not exclude one another. It is relevant to note that this spur is radial to the TPVC as is the conductive boundary between Guajara and Diego Hernandez calderas. The intersection between both lineaments is located somewhere below Pico Teide providing strong evidence for a structurally or tectonically controlled location of the volcano.

In a similar way, the morphology of the top-most conductive layer defines two separate, circular depressions (EG-D and WG-D) with a SW–NE orientation (Fig. 9). Both are exactly located between the southern LCC wall and the TPVC alignment. Both features provide evidence in favour of a vertical collapse origin for the Guajara sector. They suggest that the northern Guajara caldera wall is located below the Pico Teide and Montaña Blanca complex as postulated by Ablay and Marti (2000). Other than only by centripetal erosion, that contributed in shaping the present caldera wall (Aubert and Kieffer, 1998), the southern significant conductive barrier was never disturbed by land-slides, in stark contrast to the northern part of Tenerife. It is thus conceivable that the Guajara ring fault is located further towards

the interior of the present-day depression inside the LCC, buried and hidden under scree deposits.

To the west of Guajara caldera, a long and large conductive zone delimits Guajara with Diego Hernandez calderas. It constitutes the overlapping structural junction of both calderas as previously suggested (Aubert and Kieffer, 1998; Pous et al., 2002). Its orientation NW–SE, parallel to the Santiago del Teide ridge, provides a strong evidence for a structural or tectonic control on the caldera ring-fault location. Its southeastern-most part was characterized by a high residual gravity anomaly, already interpreted as the contact of two sub-calderas (Viera et al., 1986).

5.5. The Roques de Garcia

The Roques de Garcia formation was interpreted by Marti et al. (1994b) to represent the structural boundary between the Ucanca and Guajara calderas or at least between the western and eastern depressions of the LCC (Pous et al., 2002). Marti and Gudmundsson (2000) postulated that the Ucanca caldera may in fact extend further to the east, than previously believed, beyond the Roques de Garcia. As stated above, the print of RPC-Gua (Fig. 8) suggests that the Guajara volcanic edifice was probably divided into two volcanic systems similar to the present TPVC. The centre of the western part of this complex, inferred from RPCW-Gua (Fig. 8), was located somewhere above the current alignment of the Pico Teide vents towards the south to Guajara Peak. Our observations are in agreement with a caldera wall located to the east beyond the topographical limit of the deeply-rooted Roques de Garcia (Pous et al., 2002). We propose that rising magmas reactivated this structure to feed both the western edifice Guajara and later also the Teide vent systems. This re-use of structural weaknesses explains the structural control of vent alignment and the preferential pathways for fluid migration along fault systems (Galindo et al., 2005).

5.6. Areas and volumes of depressions

Fig. 10 summarizes the main results of this study including the estimated volume change associated with the formation of the caldera depressions. The LCC has first been divided into 3 areas (Fig. 10, inset) that include parts of the TPVC, approximately corresponding to the Ucanca (30 km^2), Guajara (34 km^2) and Diego Hernandez (38 km^2) depressions. The Roques de Garcia spur is chosen to represent the structural limit between the Ucanca and Guajara calderas although the real limit may lie further to the east. Then, we computed the volume of the resistive layer between the topography and the top of conductive layer in these three sectors. We obtained 3, 30 or 44 (see below) and 41 km^3 of resistive rocks for Ucanca, Guajara and Diego Hernandez depressions, respectively. The similar area (34 and 38 km^2) of the two latter depressions suggests that they have reached a final state related to the volcanic edifice size. Regarding the current TPVC, an identical area of −36 km^2 is circumscribed by the 2400 m.a.s.l. isohypse, i.e. the base of the TPVC. The volume of the twin-cones over 2400 m.a.s.l. is 14.3 km^3. This elevation being similar to the mean altitude of the eastern LCC caldera wall, indicates that the TPVC might be in its final stage and ready to collapse during future major eruption.

The minimum altitude of the top-most conductive layer was used to compute the volume of resistive rocks above a flat floor (Ablay and Marti, 2000). The two volumes obtained for Guajara (Fig. 10, V_{G1} and V_{G2}) highlight the uncertainty related to the bottom of Guajara caldera. While the minimum altitude of 1150 m.a.s.l. is assumed to be the bottom of Diego Hernandez caldera, the minimum altitude of Guajara (1550 m.a.s.l., Fig. 10) might be only a paleosurface contemporary to Diego Hernandez caldera collapse. The first few hundred metres of conductive rocks below Guajara may therefore be related to deposits from the Diego Hernandez collapse, implying that the top-most conductive layer marks the last vertical collapse event. This idea assumes that such an event is strongly correlated with a hydrothermal alteration peak occurring at a large scale. The real basement of Guajara caldera may in fact be at greater depth, similar to the Diego Hernandez basement, i.e. 1150 m.a.s.l. (Fig. 10). With this in mind, similar and comparable volumes of 44 km^3 and 41 km^3 are obtained for Guajara and Diego Hernandez calderas, respectively. Those volumes include the resistive rocks from the TPVC plus a non-negligible part of conductive rocks, probably resulting from erosion of the flanks of each caldera. These results increase the minimum amount of subsidence, at least for Diego Hernandez caldera, from 1100 m (Marti et al., 1997) to 1600 m.

5.7. Lateral vs. vertical collapse

The following arguments summarize our findings, which support the hypothesis of a vertical multiple collapse origin of the LCC rather than a lateral collapse origin (Ancochea et al., 1990; Marti et al., 1994a).

The morphologies of the resistivity prints have a circular shape and not, as one might expect to be the case for lateral collapses, a radial shape. This indicates that their origin is related to independent older geological formations. They are interpreted as prints of old volcanic edifices as well as indicators for caldera ring-fault structures. Deviations from a perfectly circular shape are due to hydrothermal alteration from a deeper source through preferential structural paths (Hernández et al., 2003; Galindo et al., 2005), such as caldera ring faults and conjugated faults. The resistivity prints match the locations of the Guajara and Diego Hernandez caldera depressions (Marti et al., 1994a), and are interpreted as the results of two main vertical caldera collapses. Presumably, each of them results from complex collapse processes. A giant listric fracture along which a lateral flank collapse occurred would not produce a funnel-like morphology for the top-most conductive layer and the observed resistivity distribution. This constitutes the strongest supportive argument of a vertical collapse origin of the LCC.

6. Summary and conclusions

This study shows that in volcanic areas free of EM cultural noise, high-resolution AMT surveys provide accurate and consistent maps of the resistivity distribution in a caldera

depression. Although the presence of prominent topographic structures such as the LCC wall, could affect AMT data quality and dimensionality, the results show a uniform close to 1-D behaviour. The main conclusions are summarized as follows:

1) The top-most conductive layer plunges towards the NE beneath the LCC infill, with clear evidence of three funnel-like morphologies.
2) The resistivity distributions of the first resistive and second conductive layers and the morphology of the top-most conductive layer are in agreement with the hypothesis of the destruction by three older edifices by vertical caldera collapse, discarding a lateral landslide origin for the LCC. The centres of the old volcanic edifices (Guajara and Diego Hernandez) have resistive cores, whereas the borders are more conductive. This difference in electrical properties enables their accurate location.
3) The conductivity distributions are related to the structural layout before and after the collapse of two volcanic edifices indicated by preferential pathways for hydrothermal fluid alteration. The eastwards increase in resistivity is assigned to different stages of hydrothermal alteration indicating different timescales associated with the alteration. The eastern-most sector of the LCC appears to be least affected by alteration processes and therefore points towards a younger age of the eastern LCC with respect to the central and western sectors.
4) The caldera strikes computed from the phase anisotropy reveal the sizeable effect of the TPVC on the electric structure of the entire caldera by a general radial pattern of anisotropy around the central complex. Other strikes, parallel to the southern and eastern caldera wall are dominated by the ring faults that generated the LCC.
5) To conclude, the geophysical arguments presented in this study demonstrate that the Las Cañadas caldera of Tenerife has been formed after the vertical collapse of distinct volcanic edifices over the last million years.

Acknowledgements

This project has been financed through grants from the Swiss National Science Foundation (SNSF), project no. 200020-111758/1. We gratefully acknowledge the help of Dr Joan Martí (CSIC) for field facilities, Drs François-David Vuataz, Geoffrey Ruiz and François Negro (University of Neuchâtel) for their constructive advice during the editing, Dr. Ellen Milnes for manuscript corrections and anonymous reviewers for helpful comments and improvement of the manuscript.

References

Abdel-Monem, A.N., Watkins, N., Gast, P., 1972. Potassium–argon ages, volcanic stratigraphy and geomagnetic polarity history of the Canary Islands: Tenerife, La Palma and Hierro. Am. J. Sci. 272, 805–825.

Ablay, G.J., Kearey, P., 2000. Gravity constraints on the structure and volcanic evolution of Tenerife, Canary Islands. J. Geophys. Res. 15 (B3), 5783–5796.

Ablay, G.J., Marti, J., 2000. Stratigraphy, structure, and volcanic evolution of the Pico Teide-Pico Viejo formation, Tenerife, Canary Islands. J. Volcanol. Geotherm. Res. 103, 175–208.

Aizawa, K., Yoshimura, R., Oshiman, N., Yamazaki, K., Uto, T., Ogawa, Y., Tank, S.B., Kanda, W., Sakanaka, S., Furukawa, Y., Hashimoto, T., Uyeshima, M., Ogawa, T., Shiozaki, I., Hurst, A.W., 2005. Hydrothermal system beneath Mt. Fuji volcano inferred from magnetotellurics and electric self-potential. Earth Planet. Sci. Lett. 235, 343–355.

Ancochea, E., Fúster, J.M., Ibarrola, E., Cendrero, A., Coello, J., Hernán, F., Cantagrel, J.M., Jamond, C., 1990. Volcanic evolution of the island of Tenerife (Canary Islands) in the light of new K–Ar data. J. Volcanol. Geotherm. Res. 44, 231–249.

Ancochea, E., Cantagrel, J.M., Fúster, J., Huertas, M.J., Arnaud, N.O., 1998. Comment: Vertical and lateral collapses on Tenerife (Canary Islands) and other volcanic ocean islands. Geology 26, 861–862.

Ancochea, E., Huertas, M.J., Cantagrel, J.M., Coello, J., Fúster, J.M., Arnaud, N., Ibarrola, E., 1999. Evolution of the Cañadas edifice and its implications for the origin of the Cañadas Caldera (Tenerife, Canary Islands). J. Volcanol. Geotherm. Res. 88, 177–199.

Araña, V., 1971. Litologia y estructura del Edificio Cañadas, Tenerife (Islas Canarias). Estud. Geol. XXVII, 95–135.

Araña, V., Camacho, A.G., Garcia, A., Montesimos, F.G., Blanco, I., Viera, R., Felpeto, A., 2000. Internal structure of Tenerife (Canary Islands) based on gravity, aeromagnetic and volcanological data. J. Volcanol. Geotherm. Res. 103, 43–64.

Arnaud, N.O., Huertas, M.J., Cantagrel, J.M., Ancochea, E., Fúster, J., 2001. Edades $^{39}Ar/^{40}Ar$ de los depósitos de Roques de Garcia (Las Cañadas, Tenerife). Geogaceta 29, 19–22.

Aubert, M., Kieffer, G., 1996. Schéma d'évolution d'un dôme phonolitique à la base du pic du Teide (Espagne), déduit de données géoélectriques et morphologiques. C. R. Acad. Sci., Paris 323 (II a), 645–650.

Aubert, M., Kieffer, G., 1998. Graben sector slipping hypothesis on the north-east part of the Las Canadas caldera (Teide, Tenerife, Spain). C. R. Acad. Sci., Paris 326, 87–92.

Ballestracci, R., Nishida, Y., 1987. Fracturing associated with the 1977–1978 eruption of Usu volcano, north Japan, as revealed by geophysical measurements. J. Volcanol. Geotherm. Res. 34, 107–121.

Ballestracci, R., Nougier, J., Benderitter, Y., 1985. Intermediate tectonic pattern and hydrodynamic process deduced from audiomagnetotellurics investigations on the volcanic island of Mayotte (Comores archipelago). Tectonophysics 115, 45–60.

Benderitter, Y., 1987. Recherche par géophysique d'indices peu profonds en géothermie haute énergie. Un exemple à proximité de la montagne Pelée (Martinique). Bull. Soc. Géol. Fr. III (6), 1055–1061.

Benderitter, Y., Gérard, A., 1984. Geothermal study of reunion island: audiomagnetotelluric survey. J. Volcanol. Geotherm. Res. 20, 311–332.

Bravo, T., 1962. El Circo de Las Cañadas y sus dependencias. Bol. R. Soc. Esp. Hist. Nat. 40, 93–108.

Bryan, S.E., Cas, R.A.F., Marti, J., 1998. Lithic breccias in intermediate volume phonolitic ignimbrites, Tenerife (Canary Islands): constraints on pyroclastic flow depositional processes. J. Volcanol. Geotherm. Res. 81, 269–296.

Cagniard, L., 1953. Basic theory of the magnetotelluric method of geophysical prospecting. Geophysics 18 (3), 605–635 (3).

Caloz, P., 1987. Galeries de captage d'eau sur l'île de Tenerife. Iles Canaries, Espagne. Etude des courbes de tarissements. Diploma Thesis, University of Neuchâtel, Switzerland, 67 pp.

Camacho, A.G., Viera, R., de Toro, C., 1991. Microgravimetric model of the Las Cañadas caldera (Tenerife). J. Volcanol. Geotherm. Res. 47, 75–88.

Camacho, A.G., Montesimos, F.G., Viera, R., 1996. Gravimetric structure of the Teide volcano environment. Proceedings of the Second Workshop on European Laboratory Volcanoes, Thira, Santorini Island, Greece, pp. 605–613.

Cantagrel, J.M., Arnaud, N.O., Ancochea, E., Fúster, J., Huertas, M.J., 1999. Repeated debris avalanche on Tenerife and genesis of the Las Cañadas caldera wall (Canary Islands). Geology 27 (8), 739–742.

Carracedo, J.C., 1994. The Canary Islands: an example of structural control on the growth of large oceanic-island volcanoes. J. Volcanol. Geotherm. Res. 60 (3–4), 225–241.

Coppo, N., Schnegg, P.-A., Falco, P., Costa, R., in press. Tsunamigenic risk for North Atlantic shorelines. Submitted to Earth Planet. Sci. Lett.

Courteaud, M., Ritz, M., Robineau, B., Join, J.-L., Coudray, J., 1997. New geological and hydrogeological implications of the resistivity distribution

inferred from audiomagnetotellurics over La Fournaise young shield volcano (Reunion Island). J. Hydrol. 203, 93–100.

Descloitres, M., Ritz, M., Robineau, B., Courteaud, M., 1997. Electrical structure beneath the eastern collapsed flan of Piton de la Fournaise volcano, Reunion Island: implications for the quest for groundwater. Water Resour. Res. 33 (1), 13–19.

Edgar, C.J., Wolff, J.A., Olin, P.H., Nichols, H.J., Pittari, A., Cas, R.A.F., Reiners, P.W., Spell, T.L., Martí, J., 2007. The late Quaternary Diego Hernandez Formation, Tenerife: volcanology of a complex cycle of voluminous explosive phonolitic eruptions. J. Volcanol. Geotherm. Res. 160, 59–85.

Filloux, J., 1987. Instrumentation and experimental methods for oceanic studies. In: Jacobs (Ed.), Geomagnetism. Academic Press, London.

Fischer, G., Le Quang, B.V., 1981. Topography and minimization of standard deviation in one-dimensional magnetotelluric inversion scheme. Geophys. J. R. Astron. Soc. 67, 279–292.

Fuji-ta, K., Ogawa, Y., Ichiki, M., Yamaguchi, S., Makino, Y., 1999. Audio frequency magneto-telluric (AMT) survey of Norikura Volcano in central Japan. J. Volcanol. Geotherm. Res. 90, 209–217.

Fúster, J.M., Araña, V., Brandle, J.L., Navarro, M., Alonso, U., Aparicio, A., 1968. Geología y vulcanología de las Islas Canarias, Tenerife, Special publication Instituto Lucas Mallada, CSIC. Madrid. 218 pp.

Galindo, I., Soriano, C., Martí, J., Pérez, N., 2005. Graben structure in the Las Cañadas edifice (Tenerife, Canary Islands): implications for active degassing and insights on the caldera formation. J. Volcanol. Geotherm. Res. 144 (1–4), 73–87.

Gudmundsson, A., 1988. Formation of collapse calderas. Geology 16, 808–810.

Hernández, P., Pérez, N., Salazar, J., Reimer, M., Notsu, K., Wakita, H., 2003. Radon and helium in soil gases at Cañadas caldera, Tenerife, Canary Islands, Spain. J. Volcanol. Geotherm. Res. 2721, 1–18.

Hürlimann, M., Garcia-Piera, J.-O., Ledesma, A., 2000. Causes and mobility of large volcanic landslides: application to Tenerife, Canary Islands. J. Volcanol. Geotherm. Res. 103, 121–134.

MacFarlane, D.J., Ridley, W.I., 1968. An interpretation of gravity data for Tenerife, Canary Islands. Earth Planet. Sci. Lett. 4, 481–486.

Manzella, A., Volpi, G., Zaja, A., Meju, M., 2004. Combined TEM-MT investigation of shallow-depth resistivity structure of Mt Somma–Vesuvius. J. Volcanol. Geotherm. Res. 131, 19–32.

Marinoni, L.B., Gudmundsson, A., 2000. Dykes, faults and palaeostresses in the Teno and Anaga massifs of Tenerife (Canary Islands). J. Volcanol. Geotherm. Res. 103, 83–103.

Marti, J., 1998. Comment on "A giant landslide on the northern flank of Tenerife, Canary Island" by A. B. Watts and D.G. Masson. J. Geophys. Res. 103 (B5), 9945–9947.

Marti, J., Gudmundsson, A., 2000. The Las Cañadas caldera (Tenerife, Canary Islands): an overlapping collapse caldera generated by magma-chamber migration. J. Volcanol. Geotherm. Res. 103, 161–173.

Marti, J., Mitjavila, J., Araña, V., 1994a. Stratigraphy, structure and geochronology of the Las Cañadas Caldera (Tenerife, Canary Islands). Geol. Mag. 131 (6), 715–727.

Marti, J., Ablay, G.J., Redshaw, L.T., Sparks, R.S.J., 1994b. Experimental studies of collapse calderas. J. Geol. Soc. 151, 919–929.

Marti, J., Ablay, G.J., Bryan, S., 1996. Comment on "The Canary Islands: an example of structural control on the growth of large oceanic-island volcanoes" by J.C. Carracedo. J. Volcanol. Geotherm. Res. 72, 143–149.

Marti, J., Hürlimann, M., Ablay, G.J., Gudmundsson, A., 1997. Vertical and lateral collapses on Tenerife (Canary Islands) and other volcanic oceanic islands. Geology 25, 879–882.

Masson, D.G., Watts, A.B., Gee, M.J.R., Urgeles, R., Mitchell, N.C., Le Bas, T.P., Canales, M., 2002. Slope failures on the flanks of the western Canary Islands. Earth-Sci. Rev. 57, 1–35.

Matsushima, N., Oshima, H., Ogawa, Y., Takakura, S., Satoh, H., Utsugi, M., Nishida, Y., 2001. Magma prospecting in Usu volcano, Hokkaido, Japan, using magnetotelluric soundings. J. Volcanol. Geotherm. Res. 109, 263–277.

Monteiro Santos, F.A., Trota, A., Soares, A., Luzio, R., Lourenço, N., Matos, L., Almeida, E., Gaspar, J.L., Miranda, J.M., 2006. An audio-magnetotelluric investigation in Terceira Island (Azores). J. Appl. Geophys. 59 (4), 314–323.

Müller, A., Haak, V., 2004. 3-D modeling of the deep electrical conductivity of Merapi volcano (Central Java): integrating magnetotellurics, induction vectors and the effects of steep topography. J. Volcanol. Geotherm. Res. 138, 205–222.

Navarro, J.M., Coello, J., 1989. Depressions originated by landslide processes in Tenerife. In: Araña, V. (Ed.), ESF Meeting on Canarian Volcanism, Lanzarote, pp. 150–152.

Ortiz, R., Araña, V., Astiz, M., García, A., 1986. Magnetotelluric study of the Teide (Tenerife) and Timanfaya (Lanzarote) volcanic areas. J. Volcanol. Geotherm. Res. 30 (3–4), 357–377.

Pous, J., Heise, W., Schnegg, P.-A., Muñoz, G., Marti, J., Soriano, C., 2002. Magnetotelluric study of the Las Cañadas caldera (Tenerife, Canary Islands): structural and hydrogeological implications. Earth Planet. Sci. Lett. 204, 249–263.

Revil, A., Finizola, A., Sortino, F., Ripepe, M., 2004. Geophysical investigations at Stromboli volcano, Italy: implications for ground water flow and paroxysmal activity. Geophys. J. Int. 157, 426–440.

Savin, C., Ritz, M., Join, J.-L., Bachelery, P., 2001. Hydrothermal system mapped by CSAMT on Karthala Volcano Grande Comore Island, Indian ocean. J. Appl. Geophys. 48, 143–152.

Schnegg, P.-A., 1993. An automatic scheme for 2-D magnetotelluric modelling, based on low-order polynomial fitting. J. Geomagn. Geoelectr. 45, 1039–1043.

Schnegg, P.-A., 1997. Electrical structure of Plaine des Sables caldera, Piton de la Fournaise volcano (Reunion Island). Ann. Geofis. XL (2), 305–317.

Simpson, F., Bahr, K., 2005. Practical Magnetotellurics. Cambridge University Press, Cambridge. 254 pp.

Swift, C.M., 1967. A Magnetotelluric Investigation of an Electrical Conductivity Anomaly in the Southwestern United States, Cambridge, Massachusetts. .

Tournerie, B., Chouteau, M., Marcotte, D., 2007. Magnetotelluric static shift: estimation and removal using the cokriging method. Geophysics 72 (1), F25–F34. doi:10.1190/1.2400625.

Viera, R., Toro, C., Araña, V., 1986. Microgravimetric survey in the caldera of Teide, Tenerife, Canary Islands. Tectonophysics 130, 249–257.

Volpi, G., Manzella, A., Fiordelisi, A., 2003. Investigation of geothermal structures by magnetotellurics (MT): an example from the Mt Amiata area, Italy. Geothermics 32, 131–145.

Vozoff, K., 1991. The magnetotelluric method. In: Nabighian, M. (Ed.), Electromagnetic Methods in Geophysics. SEG, Tulsa, Oklahoma, pp. 641–711.

Walter, T.R., Schmincke, H.-U., 2002. Rifting, recurrent landsliding and Miocene structural reorganization on NW-Tenerife (Canary Islands). Int. J. Earth Sci. 91, 615–628.

Walter, T.R., Troll, V.R., 2001. Formation of caldera periphery faults: an experimental study. Bull. Volcanol. 63, 191–203.

Walter, T.R., Troll, V.R., 2003. Experiments on rift zone evolution in unstable volcanic edifices. J. Volcanol. Geotherm. Res. 127 (1–2), 107–120.

Watts, A.B., Masson, D.G., 1995. A giant landslide on the north flank of Tenerife, Canary Islands. J. Geophys. Res. 100 (B12), 24487–24498.

Watts, A.B., Masson, D.G., 1998. Reply to comment on A giant land-slide on the northern flank of Tenerife, Canary Islands, by A.B Watts and D.G. Masson. J. Geophys. Res. 103 (B5), 9948–9951.

Watts, A.B., Masson, D.G., 2001. New sonar evidence for recent catastrophic collapses of the north flank of Tenerife, Canary Islands. Bull. Volcanol. 63, 8–19.

Zlotnicki, J., Sasai, Y., Yvetot, P., Nishida, Y., Uyeshima, M., Fauquet, F., Utada, H., Takahashi, T., Donnadieu, G., 2003. Resistivity and self-potential changes associated with volcanic activity: The July 8, 2000 Miyake-jima eruption (Japan). Earth Planet. Sci. Lett. 205, 139–154.